Intramolecular charge transfer of 4-(dimethylamino)benzonitrile probed by time-resolved fluorescence and transient absorption: No evidence for two ICT states and a $\pi\sigma^*$ reaction intermediate

Klaas A. Zachariasse,[1,a)] Sergey I. Druzhinin,[1] Sergey A. Kovalenko,[2] and Tamara Senyushkina[1]
[1]*Max-Planck-Institut für biophysikalische Chemie, Spektroskopie und Photochemische Kinetik, 37070 Göttingen, Germany*
[2]*Institut für Chemie, Humboldt Universität zu Berlin, Brook-Taylor Strasse 2, 12489 Berlin, Germany*

(Received 9 October 2009; accepted 10 November 2009; published online 10 December 2009)

For the double exponential fluorescence decays of the locally excited (LE) and intramolecular charge transfer (ICT) states of 4-(dimethylamino)benzonitrile (DMABN) in acetonitrile (MeCN) the same times τ_1 and τ_2 are observed. This means that the reversible LE$\rightleftarrows$ICT reaction, starting from the initially excited LE state, can be adequately described by a two state mechanism. The most important factor responsible for the sometimes experimentally observed differences in the nanosecond decay time, with $\tau_1(\mathrm{LE}) < \tau_1(\mathrm{ICT})$, is photoproduct formation. By employing a global analysis of the LE and ICT fluorescence response functions with a time resolution of 0.5 ps/channel in 1200 channels reliable kinetic and thermodynamic data can be obtained. The arguments presented in the literature in favor of a $\pi\sigma^*$ state with a bent CN group as an intermediate in the ICT reaction of DMABN are discussed. From the appearance of an excited state absorption (ESA) band in the spectral region between 700 and 800 nm in MeCN for *N*,*N*-dimethylanilines with CN, Br, F, CF_3, and C(=O)OC_2H_2 *p*-substituents, it is concluded that this ESA band cannot be attributed to a $\pi\sigma^*$ state, as only the C–C≡N group can undergo the required 120° bending. © *2009 American Institute of Physics*. [doi:10.1063/1.3270165]

I. INTRODUCTION

4-(dimethylamino)benzonitrile (DMABN) in the singlet excited state undergoes a reversible reaction from the initially populated locally excited (LE) state to the intramolecular charge transfer (ICT) state. This reaction takes place in sufficiently polar solvents, from the slightly polar toluene and diethyl ether to the strongly polar acetonitrile (MeCN) and methanol. In nonpolar alkanes such as *n*-hexane or cyclohexane, an ICT reaction does not occur to an appreciable extent.[1–7]

The principal point of discussion since now more than 35 years in connection with the ICT reaction of DMABN is the molecular structure of its ICT state, in particular the twist angle[7] of the dimethylamino group with respect to the benzonitrile moiety and hence the degree of electronic coupling[8] between these two subgroups. This discussion has been based on experimental[1–8] or on purely computational[9–15] arguments. The computations with DMABN were basically carried out for the gas phase, in which an ICT reaction does not take place.[16,17] Until recently, two ICT structures seemed to have survived from the surprisingly large number of configurations and reaction models suggested in the literature:[7] one with a fully (90°) twisted[7] dimethylamino group (TICT) and the other with a planar[6,18–20] ICT (PICT) structure. The difference between these two models resides mainly in the extent of electronic coupling between the subgroups of DMABN, smaller for TICT (principle of minimum overlap) than for PICT. This means that a configuration in which the dimethylamino group is twisted over, e.g., 60° is not a TICT state in the classical sense.[8]

Experimental support for the TICT hypothesis has been supposed to come from the similarity of the ICT transient absorption spectrum of DMABN[4,21–26] (maxima at 315 and 425 nm in MeCN)[23] with that of the benzonitrile radical anion (maxima at 314 and 403 nm in dimethylformamide,[27] 317 and 405 nm in methyltetrahydrofuran[28] at 77 K). It should be noted, however, that similar absorption spectra are observed for the radical anions of a variety of benzontriles with different parasubstituents.[27] Also the ICT absorption spectrum of the planarized DMABN derivative 1-*tert*-butyl-6-cyano-1,2,3,4-tetrahydroquinoline (NTC6) (maxima <334 and 460 nm)[8] is comparable with that of DMABN and the benzonitrile anion. Evidence for an ICT state with a perpendicular dimethylamino group can therefore not be derived from these excited state absorption (ESA) spectra.

Experimental support for the PICT model came from the PICT state derived from picosecond x-ray crystal analysis of 4-(diisopropylamino)benzonitrile (DIABN).[20] The model was also supported by the finding that the planarized NTC6 shows efficient and fast ICT in *n*-hexane and MeCN.[6,8] In discussing the significance of this observation,[29,30] it was stated that the planarized structure of NTC6 in the ground state is not a compelling confirmation of a PICT state, as the six-membered exocyclic ring of NTC6 may not be rigid. This assumption was based on calculations indicating that in the

a)Electronic mail: kzachar@gwdg.de.

ICT state of NTC6 the conjugation of the six C atoms in the phenyl ring was broken because of the pyramidal configuration of the ring carbon to which the amino nitrogen is attached.[31,32] For the ICT state of DMABN, a similar distorted pyramidal phenyl ring structure was calculated.[9] NTC6, however, has an ICT ESA spectrum resembling the absorption spectrum of the radical anion of benzonitrile,[8] similar to DMABN, as mentioned above. In the benzonitrile radical anion, all ring carbons are part of a fully delocalized phenyl moiety, as deduced from its electron spin resonance (ESR) spectrum.[33] This makes the calculated pyramidal structure unlikely as a model for the ICT state of NTC6 and DMABN. It should be taken into account that the ICT reaction in NTC6 is ultrafast, with 2.2 ps in *n*-hexane and 0.82 ps in MeCN at 22 °C,[8] precluding a substantial activation barrier for the ring distortion. The fact that with 1-methyl-6-cyano-1,2,3,4-tetrahydroquinoline (NMC6) an ICT reaction does not occur, in contrast with NTC6, has been explained by the larger energy gap between the two lowest excited singlet states $\Delta E(S_1, S_2)$ for the former molecule.[6,8]

Different from TICT and PICT, Sobolewski and Domcke had earlier advocated an ICT structure, in which not the dimethylamino substituent but rather the C≡N group of DMABN had undergone a change upon excitation, by rehybridization (bending) of the cyano group: the RICT model. From their calculations, an ICT state with a rehybridized CN group having a C–C–N angle of ~120° was obtained.[34,35] They then made the prediction that 4-(dimethylamino)phenylacetylene (DACET), a derivative of DMABN in which the CN substituent is replaced by an acetylene group, would show more efficient ICT than DMABN, even in the gas phase.[35] The ICT state of DACET likewise was thought to have a bent acetylene group, also with a C–C–C angle of ~120°. This prediction was shown not to be valid, as DACET did not undergo an ICT reaction, even in a strongly polar solvent such as acetonitrile (MeCN).[17] Later, it was shown that ICT also does not occur with DACET in *p*-dioxane/water mixtures, in which the quenching of the single LE fluorescence increases with the water content.[36,37] As it was found that a similar fluorescence quenching also takes place with NMC6, a molecule that does not show an ICT reaction as mentioned above, it was concluded that the enhanced fluorescence quenching of DACET in dioxane/water was not connected with a LE→ICT reaction.[37] The a priori possibility that the RICT (or TICT) state of DACET is in fact close in energy to the LE state but cannot be reached because of a prohibitive energy barrier on the reaction pathway to the ICT state is not experimentally falsifiable.[17,36]

Consequently, in a more advanced *ab initio* investigation, the RICT mechanism was abandoned, concluding that a RICT state in DMABN is not relevant for the ICT reaction, whether it exists at a higher energy or not.[11,38] The RICT model also was considered to be invalid on the basis of calculations of the CN stretch frequency of the DMABN ICT state in a comparison with experimental time-resolved infrared (TRIR) and resonance Raman (TR^3) data.[7,39,40] In addition, it was rejected on energetic grounds, as the RICT state was computed[7,12,13] to be higher in energy than the LE and the TICT states.

The $\pi\sigma^*$ state introduced by the RICT model was recently revived by Lim *et al.*,[21,22,29,41,42] who presented calculations from which they concluded that the state (bent C–C≡N group) is a key intermediate for DMABN in MeCN on the reaction pathway to the ICT state. Both states have a similar calculated dipole moment of around 16 D.[22] Later, the $\pi\sigma^*$ state only appeared in one of two reaction pathways starting from the initially excited $S_2(\pi\pi^*, L_a)$ Franck–Condon (FC) state, as an intermediate connecting to a dark TICT state. This pathway was supposed to run parallel to the second kinetically independent LE→ICT reaction, with two fluorescing states (*vide infra*).[21]

As the essence of the RICT hypothesis, as well as of Lim's $\pi\sigma^*$ mechanism, is the rehybridization (bending) of the C–C≡N or the C–C≡C group, the RICT and $\pi\sigma^*$ models are not applicable to electron donor(D)/acceptor(A) molecules with an A substituent different from C≡N or C≡C. Examples of such A/D molecules for which an ICT reaction occurs, are 4-(dialkylamino)benzenes with C(=O)OR, C(=O)R, C(=O)NR_2, and CF_3 as the para-substituent,[7,43] and also *N*-phenylpyrrole (PP),[44] 4-fluoro-*N*-phenylpyrrole (PP4F),[45] fluorazene (FPP),[44] 4-fluorofluorazene (FPP4F)[45] and DMABN derivatives[7] in which the benzonitrile moiety is replaced by pyridine or pyrimidine.

In the present paper, the reported difference between the nanosecond decay times τ_1(LE) and τ_1(ICT) and also the proposed $\pi\sigma^*$ ICT reaction intermediate will be discussed.

II. EXPERIMENTAL METHODS

The details of the picosecond single photon counting (SPC) and transient absorption experiments have been published previously.[23] The synthesis of aldehyde-free DMABN (Ref. 46) and 3,5-dimethyl-4-(dimethylamino)benzonitrile (MMD)[2] has been described elsewhere. The synthesis of 2,6-dimethyl-4-fluoro-*N*,*N*-dimethylaniline (MMF), 2,6-dimethyl-4-bromo-*N*,*N*-dimethylaniline (MMBr), 2,6-dimethyl-4-trifluoromethyl-*N*,*N*-dimethylaniline ($MMCF_3$), and 3,5-dimethyl-4-dimethylamino-benzoic acid ethyl ester (MME) will be published separately. For all compounds, HPLC was the last purification step, except for a number of experiments in which DMABN (Aldrich) was used as received. The solutions employed for the fluorescence decay measurements had an optical density of around 1 at the excitation wavelength (272 nm). The solutions were deoxygenated by bubbling with N_2 for 15 min, unless otherwise indicated.

III. RESULTS AND DISCUSSION

A. Fluorescence decays of DMABN in MeCN

The fluorescence spectrum of DMABN in MeCN consists of two emission bands, originating from the LE and the ICT state (Fig. 1), with an experimental ICT/LE fluorescence quantum yield ratio $\Phi'(ICT)/\Phi(LE)$ of 39.8 at 25 °C.[23] The double exponential LE and ICT fluorescence decays i_f(LE) and i_f(ICT) of DMABN in MeCN at 25 °C have the same decay times: $\tau_1 = 3800$ ps and $\tau_2 = 4.1$ ps [Eqs. (1)–(4)], determined by global analysis, although τ_2(ICT) is not well-

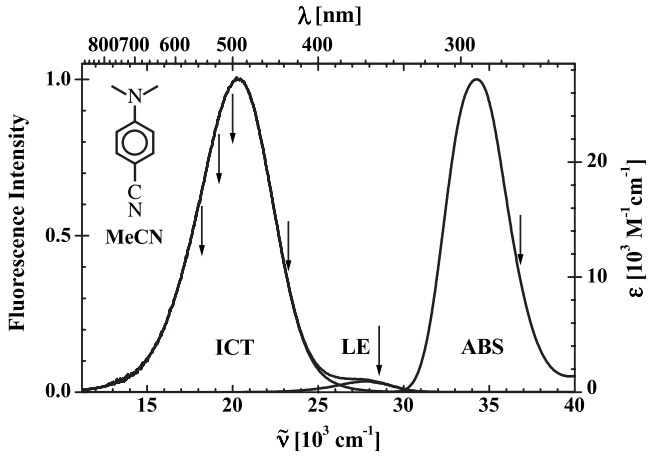

FIG. 1. Fluorescence and absorption spectra of DMABN in acetonitrile (MeCN) at 25 °C. The molar extinction coefficient is indicated on the right hand axis. The fluorescence spectrum of DMABN in MeCN is separated into its LE and ICT components, by using the LE fluorescence spectrum of 4-(methylamino)benzonitrile (MABN). The arrows indicate the excitation wavelength (272 nm) and the emission wavelengths for the decays listed in Table I.

defined for DMABN/MeCN, see below. In the experiments of Ref. 23, the fluorescence signal is measured simultaneously at two time scales (0.5 and 10 ps/channel), increasing the overall accuracy of the two vastly different decay times.

The time resolution of our picosecond SPC measurements is better than 3 ps. This time resolution is reached by deconvolution of the LE and ICT fluorescence decays with the stable excitation pulse (instrument response function ~18 ps). The short decay time τ_2 of 4.1 ps at 25 °C is smoothly embedded in a series of measurements from −45 °C (τ_2=7.7 ps) to 75 °C (τ_2=3.3 ps), which documents its accuracy and reliability.[23] Moreover, a decay time τ_2=4.07 ps at 22 °C was obtained from femtosecond transient absorption measurements, in agreement with the SPC results.[23] Therefore, the time resolution of our SPC measurements is fully adequate to test the validity of the LE⇄ICT reaction mechanism of DMABN in MeCN, contrary to what was claimed in Ref. 21.

$$i_f(\mathrm{LE}) = A_{11}\exp(-t/\tau_1) + A_{12}\exp(-t/\tau_2). \quad (1)$$

$$i_f(\mathrm{ICT}) = A_{21}\exp(-t/\tau_1) + A_{22}\exp(-t/\tau_2). \quad (2)$$

$$A = A_{12}/A_{11}. \quad (3)$$

$$A_{21} = -A_{22}. \quad (4)$$

B. Experimental reasons for different nanosecond decay times τ_1(LE) and τ_1(ICT)

One of the reasons for the opinion of Lim *et al.*[21] that the actual mechanism of the ICT reaction in DMABN may be far more complex than previously assumed, is their observation of different nanosecond LE and ICT fluorescence decay times τ_1 for dialkylaminobenzonitriles, τ_1(LE) being smaller than τ_1(ICT). This was taken as the main experimental support for their $\pi\sigma^*$ ICT mechanism. As mentioned in the previous section, the same decay times τ_1(LE) and τ_1(ICT) are obtained from our experiments of DMABN in MeCN at 25 °C. The ICT reaction is interpreted as following scheme 1, where $(L_a, \pi\pi^*)^{FC}$ and $(L_b, \pi\pi^*)^{FC}$ stand for the S_2 and S_1 FC states reached by light absorption. By relaxation and internal conversion from $(L_a, \pi\pi^*)^{FC}$ as well as from $(L_b, \pi\pi^*)$,^{FC} the equilibrated LE state is reached, the ICT precursor (scheme 1).[23]

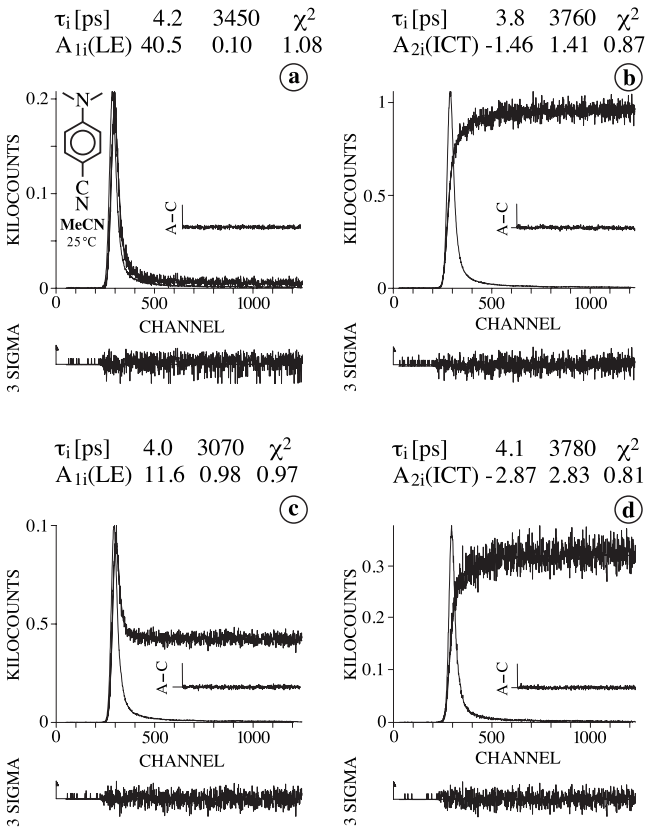

FIG. 2. Fluorescence decays of deaerated solutions of DMABN in MeCN at 25 °C [Eqs. (1)–(4)]. (a) LE decay (350 nm) for a fresh solution, with τ_1(LE)=3450 ps, τ_2(LE)=4.2 ps, and $A=A_{12}/A_{11}$=405 [Eq. (3)]. (b) ICT decay (520 nm) for a fresh solution [similar to (a)], with τ_1(ICT) =3760 ps, τ_2(LE)=3.8 ps, and A_{22}/A_{21}=−1.04 [Eq. (4)]. (c) LE decay (350 nm) for a solution after prolonged irradiation, with τ_1(LE)=3070 ps, τ_2(LE)=4.0 ps, and $A=A_{12}/A_{11}$=11.8. (d) ICT decay (520 nm) for a solution after prolonged irradiation [similar to (c)], with τ_1(ICT)=3780 ps, τ_2(ICT)=4.1 ps, and A_{22}/A_{21}=−1.01. The shortest decay time is listed first. The weighted deviations sigma, the autocorrelation functions A–C and the values for χ^2 are also indicated. Excitation wavelength: 272 nm. Time resolution: 0.496 ps/channel with a time window of 1200 effective channels.

$$(L_a,\pi\pi^*)^{FC} \xrightarrow{h\nu} (L_b,\pi\pi^*)^{FC} \longrightarrow LE \rightleftharpoons ICT$$

Upon irradiation of DMABN in solution, however, 4-(methylamino)benzonitrile (MABN) is produced as one of the photoproducts,[47] leading to a decrease in the LE amplitude ratio $A=A_{12}/A_{11}$ [Eq. (3)] from 405 to 11.8 and a shortening of τ_1(LE) from 3450 to 3070 ps, see Figs. 2(a) and 2(c). As the LE fluorescence of DMABN in MeCN is strongly quenched by the ICT reaction, by a factor of around 300 at 25 °C,[23] whereas MABN (similar fluorescence spectrum) does not undergo such a quenching, a few per mille of MABN photoproduct is sufficient for a contribution comparable to that of DMABN in the spectral range of its LE

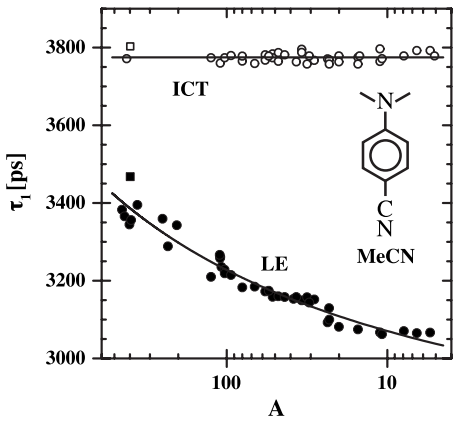

FIG. 3. The nanosecond fluorescence decay times τ_1(LE) at 350 nm and τ_1(ICT) at 520 nm of deaerated DMABN in MeCN at 25 °C as a function of the LE amplitude ratio A [Eq. (3)]. The rectangular data points come from Ref. 23. The variation in A has been achieved by increasing the duration of the laser irradiation, which leads to photochemical degradation of DMABN, see text.

fluorescence. As the photoproduct does not fluoresce at the wavelength (520 nm) at which the ICT emission is measured,[47] there is no influence of irradiation duration on τ_1(ICT), see Figs. 2(b) and 2(d) with 3760 and 3780 ps for τ_1(ICT).

The decrease in τ_1(LE) when the LE amplitude ratio A becomes smaller, i.e., with increasing duration of laser irradiation, develops smoothly, as shown in Fig. 3.

C. Influence of DMABN purity and presence of oxygen

In order to investigate possible other factors influencing the accuracy of the experimental fluorescence decay times of DMABN in MeCN, the decays were measured with solutions of DMABN as received from Aldrich with and without removal of oxygen (Table I).

A fresh deaerated solution of DMABN (Aldrich) in MeCN measured at 350 nm (LE fluorescence, Fig. 1) has the decay times τ_2(LE)=4.4 ps and τ_1(LE)=3300 ns, with A =160. In an aerated solution with τ_2(LE)=4.5 ps, the presence of oxygen leads to a decrease in τ_1(LE) to 3010 and of A to 78 (Table I). The decay time τ_1(ICT) of the ICT fluorescence in deaerated solutions at three different emission wavelengths, see Fig. 1, 3660 ps (500 and 520 nm) and 3630 ps (550 nm) is longer than τ_1(LE) due to the presence of photoproduct under the LE fluorescence spectrum. At intermediate emission wavelengths 430 and 470 nm, the overlap of LE and ICT fluorescence leads to more complicated decays, see Fig. 1 and Table I. Photoproduct formation remains the most important factor in reducing τ_1(LE). Its influence nevertheless is relatively small: 3010 ps without oxygen removal, 3330 ps for DMABN from Aldrich (not HPLC) in deaerated MeCN (Table I).

D. Extreme situation with DMABN in MeCN. Different accuracies of LE and ICT decay times

With the double exponential LE and ICT fluorescence decays of DMABN in MeCN at 25 °C, a rather extreme situation is encountered. The two decay times τ_1 (3800 ps) and τ_2 (4.1 ps) differ by a factor of about 1000. Moreover, the LE amplitude ratio $A=A_{12}/A_{11}$ [Eq. (3)] is very large, being equal to 516, when photoproduct formation does not interfere. The ICT amplitude ratio, on the contrary, A_{22}/A_{21} =−1.0 [Eq. (4)].[23] The accuracy with which the two vastly different decay times τ_2 and τ_1 can be determined from the double exponential decays is therefore not the same for the LE as compared with the ICT fluorescence response functions and it also strongly depends on the time resolution (time per channel in the SPC experiments). As an additional complication, the determination of the τ_1(LE) is difficult due to the large value (see above) of the ratio A, making it ex-

TABLE I. Fluorescence decay times τ_2 and τ_1 and amplitude ratios A_{12}/A_{11} (LE) and A_{22}/A_{21} (ICT) [Eqs. (1)–(4)] for DMABN in acetonitrile at 25 °C, from SPC experiments, measured at different emission wavelengths. See text and Fig. 1.

	τ_2(LE) (ps) (nm)	τ_1(LE) (ps) (nm)	τ_2(ICT) (ps) (nm)	τ_1(ICT) (ps) (nm)	A_{12}/A_{11}(LE) [Eq. (3)]	A_{22}/A_{21}(ICT) [Eq. (4)]
Global analysis[a]	4.1[b] (350)	3800[b] (350)	4.1 (520)	3800 (520)	390	−0.98
LE and ICT[c]	4.2	3450	3.8	3760	405	−1.04
LE and ICT[b]	4.0	3070	4.1	3780	12	−1.01
Aldrich aerated (O_2)	4.5 (350)	3010 (350)	5 (520)	3490 (520)	78	−0.99
Aldrich deaerated	4.4 (350)	3330 (350)			160	
			4.3 (430)	3660 (430)[d]	6.3[d]	
			2 (470)	3660 (470)[e]		−1.74[e]
			4 (500)	3660 (500)		−1.00
			3 (520)	3660 (520)		−0.94
			4 (550)	3630 (550)		−0.95

[a]From a global analysis of LE and ICT decays of a fresh solution, with a minor amount of photoproduct (Ref. 23).
[b]After prolonged laser irradiation [Figs. 2(c) and 2(d)], with a relatively large amount of photoproduct, see Ref. 47.
[c]Fresh solution [Figs. 2(a) and 2(b)].
[d]Influence of overlap of the LE fluorescence with the ICT emission.
[e]Value different from −1.0 [Eq. (4)], because of overlap of ICT fluorescence with LE emission and too low value of τ_2.

tremely sensitive to small amounts of photoproduct (MABN) or other impurities, as shown in Figs. 1 and 2.

The short time τ_2 is well-established in the LE decay, again because of its large amplitude A ($A=393$ under experimental conditions, starting with a fresh solution).[23] In the double exponential ICT response function, the contribution $A_{22}\tau_2/(A_{21}\tau_1+A_{22}\tau_2)$ of τ_2 to the overall ICT decay is very small, about equal to the ratio τ_2/τ_1. It is therefore difficult to obtain an accurate value for τ_2 from an analysis of the ICT response function alone. With DMABN in MeCN at 25 °C, the best option clearly is to make a global analysis of the LE and ICT decays: τ_1(ICT) stabilizes τ_1(LE), whereas the τ_2(ICT) is fixed by τ_2(LE).[23]

For fluorescence decays of DMABN and derivatives in other solvents less polar than MeCN, τ_2/τ_1 is larger and A_{12}/A_{11} is smaller, making the LE and ICT decay analysis much less problematic. Examples are DMABN in toluene, *p*-dioxane, and diethyl ether.[2,3,8,37,48–50] In all these cases, the same times τ_2 and τ_1 are found for the LE as well as the ICT decays, which shows that the two state mechanism scheme 1 is fully applicable for the ICT reaction of DMABN, irrespective of solvent polarity.

E. Influence of τ_1(LE) shortening on global LE/ICT analysis at 10 ps/channel

For DMABN in MeCN at 25 °C with a time resolution of 10 ps/channel in 1900 channels [Fig. 4(a)], τ_1(ICT) is well-defined. This is not the case for τ_2(ICT), which becomes uncertain (no negative amplitude) because of its small contribution to the total response function at this relatively low time resolution. From the LE decay curve [Fig. 4(b)], τ_1(LE) can be determined with sufficient accuracy at this time resolution, which enables the identification of changes in the decays due to photoproduct formation. In a global LE+ICT analysis at 0.5 ps/channel (time window 0.6 ns) this is not possible,[23] but it becomes clear at 10 ps/channel (time window 20 ns). Under these conditions, as seen from the error functions in Fig. 4(a), the global analysis is not perfect, different from what is shown in Fig. 4 of Ref. 23 with 0.5 ps/channel. This is caused by the fact that, due to photoproduct formation as mentioned above, τ_1(LE)=3450 ps is smaller than the τ_1(ICT) of 3780 ps, which time is not affected by laser irradiation. The influence of time resolution on the accuracy of global analysis of LE and ICT fluorescence response functions is discussed in the following section by employing simulated decay curves at two time resolutions.

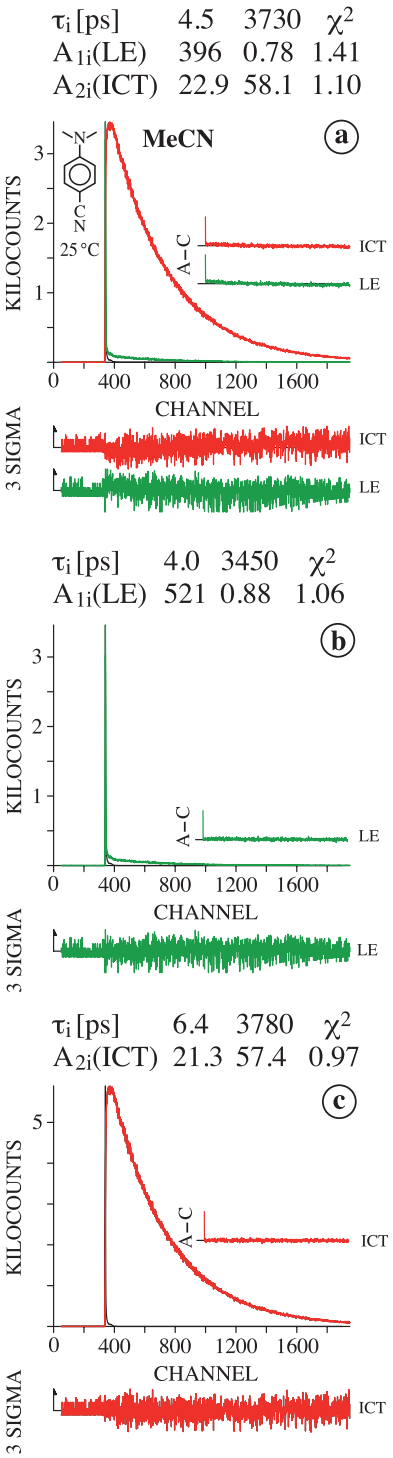

FIG. 4. Fluorescence response functions of DMABN in acetonitrile/MeCN at 25 °C with 10.04 ps/channel in 1900 channels. (a) Global LE+ICT analysis of the LE decay (b) and the ICT response function (c), giving τ_1(LE)=τ_1(ICT)=3730 ps. (b) LE decay, τ_1(LE)=3450 ps. (c) ICT fluorescence response function, τ_1(ICT)=3780 ps, see Eqs. (1)–(4) and text.

F. Simulated global analysis at two time resolutions. Influence of τ_1(LE)

To investigate the influence of a shortening of τ_1(LE) on the LE+ICT global analysis, artifical fluorescence response functions were created at two time resolutions, 0.5 ps/channel in 1200 channels and 10 ps/channel in 1900 channels (Fig. 5). In both cases, the short decay times τ_2(LE) and τ_2(ICT) are kept equal at 4.0 ps and τ_1(ICT)=3800 ps, whereas τ_1(LE) was varied in 100 ps steps starting from 3800 ps, to see when the quality of the global analysis became negatively affected by the decrease in τ_1(LE). As seen from a comparison of Figs. 5(a) and 5(b) with 0.5 ps/channel, the residuals and the autocorrelation function of the LE decay clearly indicates a low-quality fit for a substantial decrease to 600 ps of τ_1(LE). This means that at this time resolution the influence of a shortening of τ_1(LE) on the global analyis is not very large. For 10 ps/channel a different situation is encountered, as presented in Fig. 5(d), with a

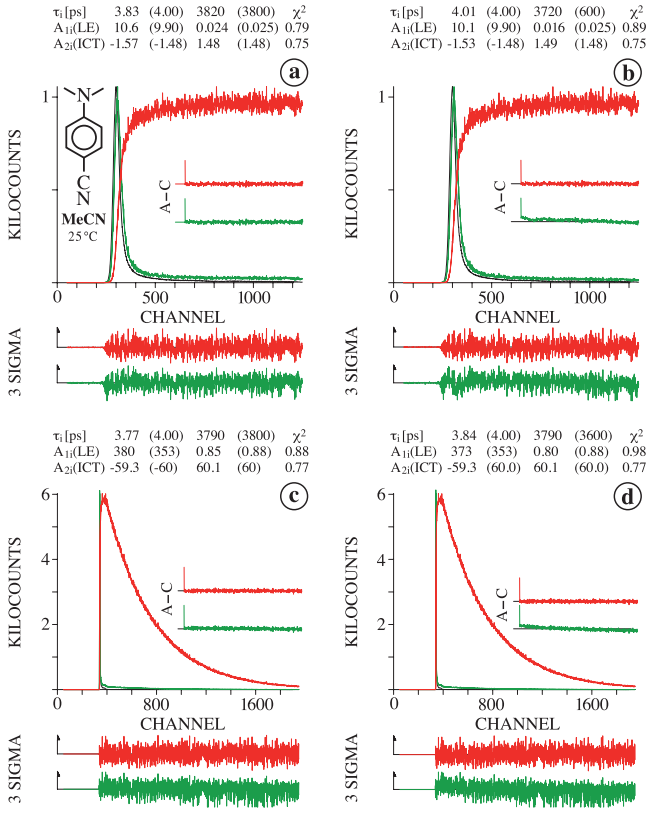

FIG. 5. Global analysis of simulated LE and ICT fluorescence response functions (SPC) of DMABN in MeCN at 25 °C for two time resolutions: 0.5 ps/channel in 1200 channels [(a) and (b)] and 10 ps/channel in 1900 channels [(c) and (d)]. For all ICT response functions, the simulation was made with τ_2=4.0 ps and τ_1=3800 ps with A_{22}/A_{21}=−1.0 [Eqs. (2) and (4)]. The LE decays in (a) and (c) have the same decay times τ_2=4.0 ps and τ_1=3800 ps, with A_{12}/A_{11}=400 [Eqs. (1) and (3)]. To show the influence of shortening of τ_1(LE) on the global analysis, τ_2=4.0 ps and τ_1=600 ps in (b) and τ_2=4.0 ps and τ_1=3600 ps in (d) were used in the simulations. These τ_1 values represent the shortest times at which a problematic LE residuals and autocorrelation functions (A–C) become clearly visible at the two time scales. See caption of Fig. 2.

significant deviation in the LE error functions already appearing for τ_1(LE)=3600 ps as compared with the perfect global fits for τ_1(LE)=3800 in Fig. 5(c). These simulations show that the problem of photoproduct formation leading to a shortening of τ_1(LE) is much less severe at 0.5 ps/channel than at 10 ps/channel, which means that LE and ICT fluorescence decays of DMABN in MeCN can be adequately measured at the shorter time scale.[23] The influence of the variation in τ_1(LE) on the ICT rate constants k_a and k_d as well as on τ_0'(ICT) (scheme 2) is found to be only minor, see Table II

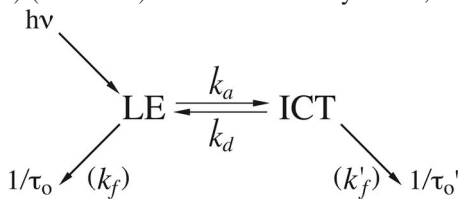

In scheme 2 and Table II, k_a and k_d are the rate constants of the forward and backward ICT reaction, τ_0(LE) and τ_0'(ICT) are the fluorescence lifetimes, and k_f(LE) and k_f'(ICT) are the radiative rate constants. For the calculation of k_a, k_d, and τ_0'(ICT) from the decay parameters τ_1, τ_2, A_{12}/A_{11}, and the lifetime τ_0(LE) of a model compound without ICT (MABN, Table II), see Ref. 23.

G. Decay times and amplitudes of DMABN in MeCN from the literature

In Table III, the decay times τ_1 and τ_2 for the LE and ICT states of DMABN in MeCN at around room temperature are listed, starting from the most recent data. It is seen that τ_1(LE), of the fluorescence decays, ranges between 2550 and 3800 ps. For τ_1 (ICT), times between 4800 ps (transient absorption) and 2900 ps (fluorescence decays) are found. The reason for these experimental differences is not known. Note that our τ_1(LE) of 3800 ps is practically the same as the first value of 3700 ps reported for this decay time.[51]

H. ICT reaction schemes with a $\pi\sigma^*$ intermediate

Lim *et al.* first assumed that for DMABN the ICT reaction started from the initially excited (L_a, $\pi\pi^*$), in fact a FC state belonging to the S_2 manifold, going from there via a dark $\pi\sigma^*_{C\equiv N}$ intermediate to the final ICT state: (L_a, pp^*) $\rightarrow ps^*_{C\equiv N} \rightarrow$ ICT.[41,42] Later, two different ICT reaction schemes involving a $\pi\sigma^*$ state (dark intermediate), scheme 3 (Ref. 22) and scheme 4 (Ref. 21), have been presented. In

TABLE II. Fluorescence decay times τ_2 and τ_1, amplitude ratios A_{12}/A_{11} (LE) and A_{22}/A_{21} (ICT) [Eqs. (1)–(4)], forward and backward ICT rate constants k_a and k_d and the ICT lifetime τ_0'(ICT) (scheme 2) derived from a global analyis of artifical LE and ICT fluorescence response functions at two time resolutions (0.496 and 10.04 ps/channel), see Fig. 5. The value of τ_1(LE) used as input in the global analysis is listed. The other input data are kept fixed: τ_2(ICT)=τ_2(LE)=4.0 ps, τ_1(ICT)=3800 ps, A_{12}/A_{11}(LE)=400, and A_{22}/A_{21}(ICT)=−1.00. These data are modeled on DMABN in acetonitrile at 25 °C (Ref. 23).For the calculation of k_a, k_d, and τ_0'(ICT) from τ_2, τ_1, and A_{12}/A_{11}, τ_0(LE)=3410 ps of the model compound MABN (no ICT) is employed.

	τ_1(LE) (ps)	τ_1 (ps)	τ_2 (ps)	A_{12}/A_{11} [Eq. (3)]	A_{22}/A_{21} [Eq. (4)]	k_a (10^9 s^{-1})	k_d (10^9 s^{-1})	τ_0'(ICT) (ns)
Fixed data[a]		3800	4.00	400	−1.00	249	0.63	3.80
Fig. 5(a)	3800	3820	3.83	442	−1.06	260	0.59	3.82
Fig. 5(b)	600	3720	4.01	631	−1.03	249	0.39	3.72
Fig. 5(c)	3800	3790	3.77	447	−0.987	264	0.59	3.79
Fig. 5(d)	3600	3790	3.84	466	−0.987	260	0.56	3.79

[a]Input data without global analysis.

TABLE III. Decay times t_2 and τ_1 and LE amplitude ratio A_{12}/A_{11} [Eq. (3)] for DMABN in acetonitrile (data for each section in the order of publication, starting with the latest).

Method	τ_2(LE) (ps) (nm)	τ_1(LE) (ps) (nm)	τ_2(ICT) (ps) (nm)	τ_1(ICT) (ps) (nm)	A_{12}/A_{11}(LE)	T (°C) or rt[a]	Reference
Upconversion	3.07 (350)		3.07 (550)			rt	21
	3.7 (350)		3.7 (500)			20	30
Transient absorption	4.33 (680)		4.3 (420)	4800 (330)		rt	21
	4.2 (680) 3.6 (480)		4.1 (410)			rt	22
	4.07 (570–970)					22	23
Fluorescence decays (SPC)		2550 (350)		2920 (470)	16[b]	rt	21
(SPC)	4.1[c] (350)	3800[b] (350)	4.1 (520)	3800 (520)	390	25	23
(SPC)	(4.6)[d] (350)	(3210)[c] (350)			9.6	25	47
(streak)	7 (355)	2600 (355)	7	2900	33	rt	52
(streak)	6 (<400)	2900 (<400)	6 (>450)	2900 (>450)	99	rt	54
(SPC)	6 (358)	3120 (358)			10	25	18
(SPC)[e]	20	3290			4.3	25	55
(streak)	<10(350)		<10(>520)	3700(>520)		20	51
(streak)	~13 (360)		~14 (465)			rt	56
TRIR[f]			4.0			rt	39
			6.4	2700		rt	5,53

[a]Room temperature.
[b]Private communication E. C. Lim.
[c]From a global analysis of LE and ICT decays of a fresh solution, with a minor amount of photoproduct (see Ref. 23). The short decay time τ_2=4.1 ps at 25 °C is smoothly embedded in a series of measurements from −45 °C (τ_2=7.7 ps) to 75 °C (τ_2=3.3 ps), which documents its accuracy and reliability.
[d]After prolonged irradiation, with a relatively large amount of photoproduct (MABN, see Ref. 47).
[e]Data obtained with the microchannel plate (MCP) Hamamatsu R1564 U-07, leading to considerably lower time resolution (pulse width ~60 ps) than that of the other SPC data in Refs. 18, 23, and 47 (30 to 18 ps) employing later MCP models (R2809U-07 and R3809U). In addition, a considerably higher laser excitation intensity was used than in later experiments, causing relatively small A values due to photochemical degradation of the dilute ($\sim 3\times 10^{-5}$ M) solutions, Ref. 55.
[f]Time-resolved infrared.

scheme 3, $L_a(\pi\pi^*)^{FC}$ is assumed to bifurcate into LE and $\pi\sigma^*_{C\equiv N}$ in less than 200 fs, the time resolution of the transient absorption experiments (scheme 3).[22]

$$(L_a,\pi\pi^*)^{FC} \begin{array}{l} \nearrow \text{LE}(\pi\pi^*) \\ \searrow \pi\sigma^*(\text{dark}) \longrightarrow \text{TICT} \end{array}$$

In scheme 4, different from scheme 3, after excitation to the FC state ($L_a, \pi\pi^*$) the reaction scheme splits into two kinetically noncommunicating pathways (no rapid population equilibration between $\pi\sigma^*$ and LE):[22] (a) LE as the precursor of ICT and (b) the dark $\pi\sigma^*$ which passes to an equally dark TICT state. No evidence is presented why this TICT state should be dark (scheme 4).

$$(L_a,\pi\pi^*)^{FC} \begin{array}{l} \nearrow \text{LE} \longrightarrow \text{ICT} \\ \searrow \pi\sigma^*(\text{dark}) \longrightarrow \text{TICT (dark)} \end{array}$$

When scheme 3 would be valid, a reversible ICT reaction as observed with DMABN (Ref. 23) could not easily be visualized, as LE would not be populated directly by the back reaction from TICT. This would result in a sum of two decays, single exponential for LE and, in principle, double expenetial for TICT, different from the double exponential LE and ICT response functions observed for DMABN in MeCN over a large temperature range.[23]

According to scheme 4, the LE and ICT fluorescence decays should be double exponential, when the LE→ICT reaction is reversible. The two dark states $\pi\sigma^*$ and TICT could only be detected by transient absorption measurements, which would also show contributions from LE and ICT, leading to a complex decay pattern for the transient absorption comprising 4 states, contrary to observation.[23]

I. Excitation wavelength dependence for $\pi\sigma^*$ reaction schemes

According to the two schemes 3 and 4 involving a $\pi\sigma^*$ state, the ratio $\Phi'(\text{ICT})/\Phi(\text{LE})$ would show an excitation wavelength dependence, as with excitation energies between the $E(S_1)$ of ($L_b, \pi\pi^*$) and $E(S_2)$ of ($L_a, \pi\pi^*$) only the S_1 LE state would be excited, going from there to $\pi\sigma^*$. With excitation energies equal to or larger than $E(S_2)$, on the other hand, two pathways would be open, leading from $S_2(L_a)$ to $\pi\sigma^*$ and then on to the final ICT state. Such an excitation wavelength dependence has, however, not been observed for DMABN in tetrahydrofuran.[43]

J. Arguments presented in favor of the $\pi\sigma^*$ intermediate

(1) The absorption maximum of the calculated highly allowed $\pi\sigma^* \rightarrow \pi\sigma^*$ excited state transient absorption was considered to be the key issue in favor of the validity of the $\pi\sigma^*$ mediated ICT mechanisms (schemes 3 and 4), as no allowed $\pi\pi^* \rightarrow \pi\pi^*$ transition between 350 and 725 nm was obtained from time-dependent density functional theory (TDDFT) calculations.[22] Only a $\pi\sigma^* \rightarrow \pi\sigma^*$ transition (633 nm, gas phase) was calculated above 500 nm, in the same spectral range as the

maxima of the strong LE excited state absorption (ESA) bands observed with DMABN in *n*-hexane (755 nm) and MeCN (710 nm).[23] The $\pi\sigma^*$ state was considered to be a dark state, which obviously complicates its experimental detection and verification. Note that very few, if any, other calculations of ESA spectra of molecules such as DMABN can be found in the literature.

(2) A second argument thought to support the $\pi\sigma^*$ ICT mechanism was seen in our observation[23] that the 710 nm LE ESA band of DMABN in MeCN exhibits a time-dependent spectral shift, whereas such a shift was not reported for the 450 nm ESA band, likewise attributed by us to LE.[22] As mentioned in Ref. 23, the time-dependent blueshift in the ESA band with a maximum around 710 nm for delay times between 0.2 and 4 ps can be fitted as the sum of a Gaussian and an exponential $(a_1 \exp(-1/2\omega^2 t^2)+a_2 \exp(-t/\tau_2))$,[23] with the following times ω^{-1} and τ_2: $\omega^{-1}=110$ fs and $\tau_2=550$ fs, having relative contributions of 0.54 and 0.46. These times and relative amplitudes are similar to those observed for the dielectric solvent relaxation of MeCN: 89 fs (0.69) and 630 fs (0.31) or 68 fs (0.70) and 600 fs (0.30). For the minor maxima around 440 nm (LE) and 425–490 nm (ICT), a time-dependent shift cannot reliably be determined, due to its relatively small absorption intensity and possible spectral overlap. In comparison, for FPP4F and PP4F, molecules with a F substituent instead of CN, only a very small shift in the ESA band around 730 nm (FPP4F) and 740 nm (PP4F), is observed when going from *n*-hexane to MeCN.[45] Our measurements for DMABN in MeCN, in contrast to what is written in Ref. 22, therefore do not demonstrate that the decay of the 450 nm transient is clearly different from that of the 700 nm transient. We in fact observe a main LE ESA maximum around 700 nm for a delay time between 0.2 and 8 ps. A maximum at 450 nm is not clearly visible, due to the overlap of a decaying LE and a rising ICT band.

(3) The third argument in favor of the intermediacy of a $\pi\sigma^*$ state,[22] that for DMABN the maximum of the 450 nm ESA band is the same in *n*-hexane (445 nm) and MeCN (440 nm), which is not so for the 700 nm ESA band (745 nm in *n*-hexane, 710 nm in MeCN), is likewise not valid, as the maxima around 450 nm are relatively weak and overlap with other bands, as discussed above. They can therefore not be determined with sufficient accuracy.

(4) Lim *et al.*[22,41] have claimed that for DMABN in *n*-hexane (only LE, no ICT) the state responsible for the 745 nm ESA maximum has a CN stretch frequency of 1467 cm^{-1}, whereas the 450 nm transient originates from a state with a CN stretch frequency of 2180 cm^{-1}. This interpretation that in picosecond time-resolved resonance Raman (TR^3) experiments[4] probing by 460 or 600 nm does not address the same state may be inconclusive, as the spectra are obtained by two different methods, Kerr-gated resonance Raman and TR^3. The authors of Ref. 4, in contrast, come to the conclusion that S_n states of similar character are resonant with LE at both 460 and 600 nm. Moreover, the same picosecond TR^3 spectrum is obtained for MABN in MeOH at 460 nm and DMABN in cyclohexane at 600 nm.[4] Reliable evidence for a $\pi\sigma^*$ state with an ESA maximum at around 700 nm is hence not provided by these Raman experiments.

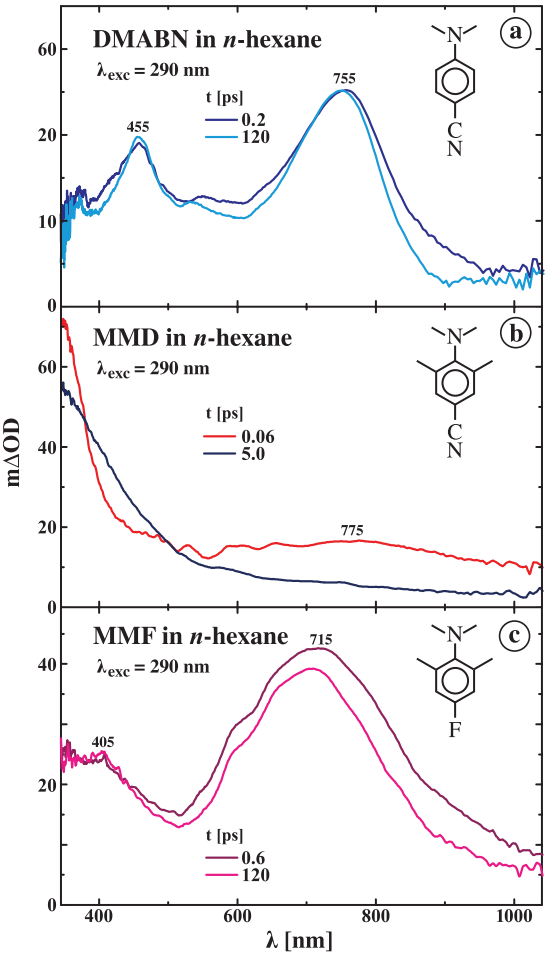

FIG. 6. ESA spectra at two pump-probe delay times of DMABN, MMD, and MMF in *n*-hexane at 22 °C. A correction for stimulated emission has been applied.

K. Transient absorption spectra

The main experimental support for the existence of a $\pi\sigma^*$ ICT intermediate with a bent –C≡N group, as discussed in a previous section, was considered to be the agreement between the maximum at 755 nm in the LE transient absorption spectrum of DMABN in *n*-hexane [Fig. 6(a)][23] and the computed $\pi\sigma^* \rightarrow \pi\sigma^*$ transition at 633 nm.[22] For the existence of this $\pi\sigma^*$ intermediate, the possibility to bend the substituent group is essential. Therefore transient absorption spectra were measured of the DMABN analogues MMD, MMBr, MMF, $MMCF_3$, and MME, for which such a bending cannot take place.

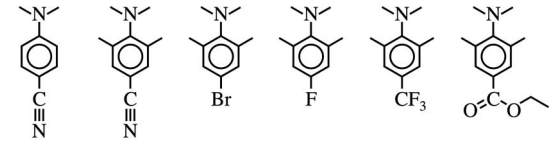

Chart 1

ESA spectra of DMABN, MMD, and MMF in *n*-hexane at 22 °C for a short and a long pump-probe delay time are presented in Fig. 6. These spectra all show a band with a maximum above 700 nm: 755 nm (DMABN), 775 nm (MMD), and 715 nm (MMF). These bands are hence attributed to the LE state. With MMD in *n*-hexane [Fig. 6(b)], the LE band decays in the subpicosecond time range (decay time 230 fs). This shows that LE is the precursor of the ICT state, contrary to the opinion expressed in Ref. 22.[57] A similar conclusion is made from the decay of the LE ESA band around 700 nm for MMD in MeCN, see Fig. 7(a). The maximum of the ESA ICT band of MMD occurs below 350 nm in *n*-hexane [Fig. 6(b)] and at about 370 nm in MeCN [Fig. 7(a)]. The observation that the halfwidth of the MMD fluorescence band decreases with increasing solvent polarity when going from *n*-pentane to MeCN, has previously been interpreted as a possible indication of dual (LE+ICT) fluorescence of MMD in *n*-hexane.[7,18,55] With DMABN and MMF in *n*-hexane an ICT reaction does not take place, as concluded from the time development of the ESA bands in Figs. 6(a) and 6(c). The slow decay found for MMF in *n*-hexane (5.5 ps) and MeCN (3.0 ps) is attributed to vibrational cooling, as in the case of DMABN and other D/A molecules.[8,23,45]

The ESA spectra of MMD, MMF, MMBr, $MMCF_3$, and MME in MeCN are presented in Fig. 7. The five compounds all show an absorption band around 700 nm. With the F, Br, CF_3, and $C(=O)OC_2H_5$ *p*-substituents, a bent structure as postulated[22] for $-C\equiv N$ is clearly not possible, as already discussed in the Introduction in connection with the observation of the dual fluorescence for such compounds. From the spectra in Fig. 6 and those in Fig. 7, it is therefore concluded that the ESA band around 700 nm obtained for DMABN in *n*-hexane and MeCN,[4,23] is likewise not a $\pi\sigma^* \rightarrow \pi\sigma^*$ transition from a state with of a bent cyano substituent suggested by Lim.

It was recently mentioned that the assignment of the 700 nm transient to the $\pi\sigma^*(C\equiv N)$ state is strongly supported by the fact that 4-(dimethylamino)benzaldehyde (DMABA) and related ketones and ethers, without a cyano group, do not exhibit an absorption around 700 nm (spectra not shown).[58] This is rather surprising, as among the D/A molecules
having a C(=O)R substituent, 5-formyl-1-methyl-indoline (FMI) in MeCN (no ICT), has a transient absorption spectrum with a maximum at about 610 nm.[7,59,60] Also 5-*N*,*N*-dimethylamino-1-indanone (DMI) in 1-propanol has a pronounced transient absorption maximum in this spectral range (shifting from 635 to 620 nm due to relaxation of the polar solvent). These bands, of molecules that do not contain a cyano group, have been attributed to the LE state.[7,59] Even

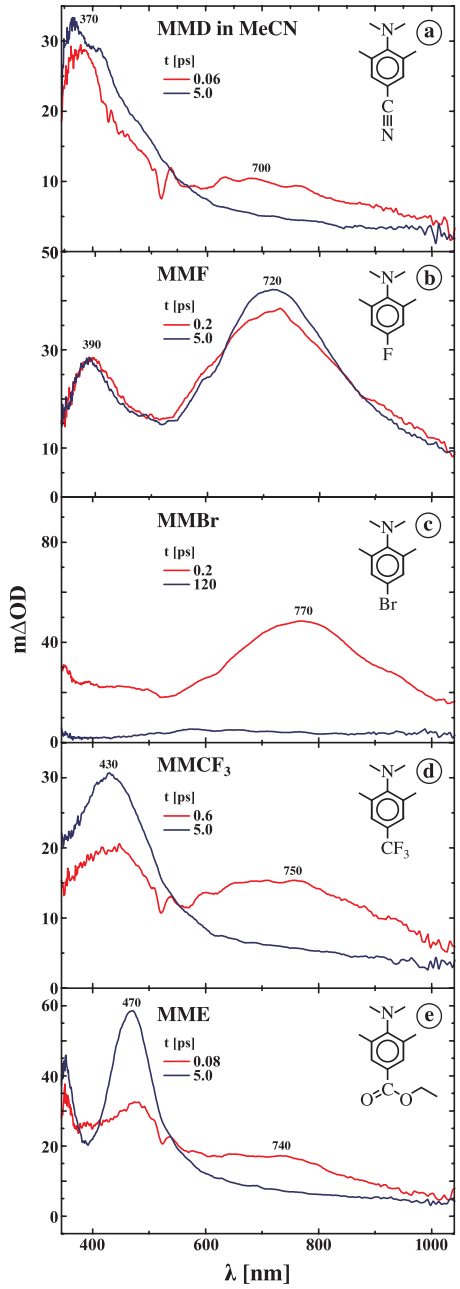

FIG. 7. ESA spectra at two pump-probe delay times of (a) MMD, (b) MMF, (c) MMBr, (d) $MMCF_3$, and MME in acetonitrile (MeCN) at 22 °C. A correction for stimulated emission has been applied.

at a pump-probe delay time of 120 ps, an ESA band is visible with DMABA and 4-(*N*,*N*-dimethylamino)acetophenone in MeCN, next to the major ICT absorption band.[59]

IV. CONCLUSIONS

For DMABN in MeCN, as well as in other solvents, the reversible ICT reaction can be adequately described by a two state mechanism involving a LE as the precursor of an ICT state (scheme 1). The double exponential LE and ICT fluorescence decays have the same decay times τ_1 and τ_2. A difference in the experimental nanosecond decay times, with $\tau_1(\mathrm{LE}) < \tau_1(\mathrm{ICT})$, can be brought about by the formation of photoproducts such as MABN upon laser irradiation. Other reasons for the appearance of this difference are the purity of

DMABN and the removal of oxygen from the solvent. When measuring the LE and ICT fluorescence decays of pure DMABN in deaerated MeCN employing a global analysis at a time resolution of 0.5 ps/channel in 1200 channels, as in Ref. 23, the influence of photoproduct formation on the kinetic [k_a, k_d, and τ_0'(ICT)] and thermodynamic (E_a, E_d, ΔH, and ΔS) analysis of the ICT reaction is negligible.

The femtosecond ESA spectra in MeCN of a series of *N*,*N*-dimethylanilines with the *p*-substituents CN, Br, F, CF_3 and $C(=O)OC_2H_5$ all contain an absorption band in the spectral region between 700 and 800 nm. From these observations it is concluded that these ESA bands can not be attributed to a $\pi\sigma^*$ state.

ACKNOWLEDGMENT

Many thanks are due to Prof. N.P. Ernsting (Humboldt University Berlin) for the use of the femtosecond absorption equipment in the investigations reported here.

[1] E. Lippert, W. Lüder, F. Moll, W. Nägele, H. Boos, H. Prigge, and I. Seibold-Blankenstein, Angew. Chem. **73**, 695 (1961).
[2] U. Leinhos, W. Kühnle, and K. A. Zachariasse, J. Phys. Chem. **95**, 2013 (1991).
[3] W. Schuddeboom, S. A. Jonker, J. M. Warman, U. Leinhos, W. Kühnle, and K. A. Zachariasse, J. Phys. Chem. **96**, 10809 (1992).
[4] C. Ma, W. M. Kwok, P. Matousek, A. W. Parker, D. Phillips, W. T. Toner, and M. Towrie, J. Phys. Chem. A **106**, 3294 (2002).
[5] W. M. Kwok, M. W. George, D. C. Grills, C. Ma, P. Matousek, A. W. Parker, D. Phillips, W. T. Toner, and M. Towrie, Angew. Chem. Int. Ed. Engl. **42**, 1826 (2003).
[6] K. A. Zachariasse, S. I. Druzhinin, W. Bosch, and R. Machinek, J. Am. Chem. Soc. **126**, 1705 (2004).
[7] Z. R. Grabowski, K. Rotkiewicz, and W. Rettig, Chem. Rev. (Washington, D.C.) **103**, 3899 (2003).
[8] S. I. Druzhinin, S. A. Kovalenko, T. Senyushkina, and K. A. Zachariasse, J. Phys. Chem. A **111**, 12878 (2007).
[9] I. Gómez, M. Reguero, M. Boggio-Pasqua, and M. Robb, J. Am. Chem. Soc. **127**, 7119 (2005).
[10] A. Köhn and C. Hättig, J. Am. Chem. Soc. **126**, 7399 (2004).
[11] W. Sudholt, A. Staib, A. L. Sobolewski, and W. Domcke, Phys. Chem. Chem. Phys. **2**, 4341 (2000).
[12] A. B. J. Parusel, G. Köhler, and S. Grimme, J. Phys. Chem. A **102**, 6297 (1998).
[13] J. Dreyer and A. Kummrow, J. Am. Chem. Soc. **122**, 2577 (2000).
[14] C. J. Jamorski and H. P. Lüthi, J. Chem. Phys. **119**, 12852 (2003).
[15] D. Rappoport and F. Furche, J. Am. Chem. Soc. **126**, 1277 (2004).
[16] R. Daum, S. Druzhinin, D. Ernst, L. Rupp, J. Schroeder, and K. A. Zachariasse, Chem. Phys. Lett. **341**, 272 (2001).
[17] K. A. Zachariasse, M. Grobys, and E. Tauer, Chem. Phys. Lett. **274**, 372 (1997).
[18] K. A. Zachariasse, M. Grobys, Th. von der Haar, A. Hebecker, Yu. V. Il'ichev, Y.-B. Jiang, O. Morawski, and W. Kühnle, J. Photochem. Photobiol., A **102**, 59 (1996); **115**, 259 (1998).
[19] K. A. Zachariasse, Chem. Phys. Lett. **320**, 8 (2000).
[20] S. Techert and K. A. Zachariasse, J. Am. Chem. Soc. **126**, 5593 (2004).
[21] T. Gustavsson, P. B. Coto, L. Serrano-Andrés, T. Fujiwara, and E. C. Lim, J. Chem. Phys. **131**, 031101 (2009).
[22] J.-K. Lee, T. Fujiwara, W. G. Kofron, M. Z. Zgierski, and E. C. Lim, J. Chem. Phys. **128**, 164512 (2008).
[23] S. I. Druzhinin, N. P. Ernsting, S. A. Kovalenko, L. Pérez Lustres, T. A. Senyushkina, and K. A. Zachariasse, J. Phys. Chem. A **110**, 2955 (2006).
[24] W. M. Kwok, C. Ma, M. W. George, D. C. Grills, P. Matousek, A. W. Parker, D. Philips, W. T. Toner, and M. Towrie, Phys. Chem. Chem. Phys. **5**, 1043 (2003).
[25] T. Okada, M. Uesugi, G. Köhler, K. Rechthaler, K. Rotkiewicz, W. Rettig, and G. Grabner, Chem. Phys. **241**, 327 (1999).
[26] T. Okada, N. Mataga, and W. Baumann, J. Phys. Chem. **91**, 760 (1987).
[27] S. U. Pedersen, T. B. Christensen, T. Thomasen, and K. Daasbjerg, J. Electroanal. Chem. **454**, 123 (1998).
[28] T. Shida, *Electronic Absorption Spectra of Radical Ions* (Elsevier, Amsterdam, 1988).
[29] M. Z. Zgierski, T. Fujiwara, and E. C. Lim, Chem. Phys. Lett. **463**, 289 (2008).
[30] A. Pigliucci, E. Vauthey, and W. Rettig, Chem. Phys. Lett. **469**, 115 (2009).
[31] C. Hättig, A. Hellweg, and A. Köhn, J. Am. Chem. Soc. **128**, 15672 (2006).
[32] I. Gómez, Y. Mercier. and M. Reguero, J. Phys. Chem. A **110**, 11455 (2006).
[33] G. R. Stevenson, G. C. Wehrmann, and R. C. Reiter, J. Phys. Chem. A **95**, 901 (1991).
[34] A. L. Sobolewski and W. Domcke, Chem. Phys. Lett. **250**, 428 (1996).
[35] A. L. Sobolewski and W. Domcke, Chem. Phys. Lett. **259**, 119 (1996).
[36] N. Chattopadhyay, C. Serpa, M. M. Pereira, J. S. de Melo, and L. G. Arnaut, J. Phys. Chem. A **105**, 10025 (2001).
[37] K. A. Zachariasse, T. Yoshihara, and S. I. Druzhinin, J. Phys. Chem. A **106**, 6325 (2002).
[38] A. L. Sobolewski, W. Sudholt, and W. Domcke, J. Phys. Chem. A **102**, 2716 (1998).
[39] C. Chudoba, A. Kummrow, J. Dreyer, J. Stenger, E. T. J. Nibbering, T. Elsaesser, and K. A. Zachariasse, Chem. Phys. Lett. **309**, 357 (1999).
[40] W. M. Kwok, C. Ma, D. Phillips, P. Matousek, A. W. Parker, and M. Towrie, J. Phys. Chem. A **104**, 4188 (2000).
[41] M. Z. Zgierski and E. C. Lim, J. Chem. Phys. **121**, 2462 (2004).
[42] M. Z. Zgierski and E. C. Lim, J. Chem. Phys. **122**, 111103 (2005).
[43] V. A. Galievsky and K. A. Zachariasse, Acta Phys. Pol. A **112**, S-39 (2007).
[44] T. Yoshihara, S. I. Druzhinin, and K. A. Zachariasse, J. Am. Chem. Soc. **126**, 8535 (2004).
[45] S. I. Druzhinin, S. A. Kovalenko, T. A. Senyushkina, A. Demeter, R. Januskevicius, P. Mayer, D. Stalke, R. Machinek, and K. A. Zachariasse, J. Phys. Chem. A **113**, 9304 (2009).
[46] A. Demeter and K. A. Zachariasse, Chem. Phys. Lett. **380**, 699 (2003).
[47] S. I. Druzhinin, V. A. Galievsky, and K. A. Zachariasse, J. Phys. Chem. A **109**, 11213 (2005).
[48] Th. von der Haar, A. Hebecker, Yu. V. Il'ichev, W. Kühnle, and K. A. Zachariasse, AIP Conf. Proc. **364**, 295 (1996).
[49] Yu. V. Il'ichev, W. Kühnle, and K. A. Zachariasse, J. Phys. Chem. A **102**, 5670 (1998).
[50] A. Demeter, S. Druzhinin, M. George, E. Haselbach, J.-L. Roulin, and K. A. Zachariasse, Chem. Phys. Lett. **323**, 351 (2000).
[51] D. Huppert, S. D. Rand, P. M. Rentzepis, P. F. Barbara, W. S. Struve, and Z. R. Grabowski, J. Chem. Phys. **75**, 5714 (1981).
[52] E. Iwase, A. Tomioka, H. Saigusa, and M. Yagi, Phys. Chem. Chem. Phys. **6**, 3852 (2004).
[53] D. Phillips, IEEE Spectrum **15**, 8 (2002).
[54] P. Changenet, P. Plaza, M. M. Martin, and Y. H. Meyer, J. Phys. Chem. A **101**, 8186 (1997).
[55] K. A. Zachariasse, Th. von der Haar, A. Hebecker, U. Leinhos, and W. Kühnle, Pure Appl. Chem. **65**, 1745 (1993).
[56] Y. Takagi, M. Sumitani, and K. Yoshihara, Rev. Sci. Instrum. **52**, 1003 (1981).
[57] K. A. Zachariasse, S. I. Druzhinin, P. Mayer, S. A. Kovalenko, and T. Senyushkina, Chem. Phys. Lett. **484**, 28 (2009).
[58] T. Fujiwara, J.-K. Lee, M. Z. Zgierski, and E. C. Lim, Phys. Chem. Chem. Phys. **11**, 2475 (2009).
[59] C. Rullière, Z. R. Grabowski, and J. Dobkowski, Chem. Phys. Lett. **137**, 408 (1987).
[60] J. Dobkowski, Z. R. Grabowski, J. Jasny, and Z. Zieliński, Acta Phys. Pol. A **88**, 455 (1995).